Proceedings of the ASME 2024
International Mechanical Engineering Congress and Exposition
IMECE2024
November 17-21, 2024, Oregon Convention Center, Portland, OR

IMECE2024-144794

A NOVEL MODEL FOR HEART BEATING RHYTHMS

Xinya Wang and **Yeyin Xu**[1]
School of Aerospace Engineering and
State Key Laboratory for Strength and Vibration of Mechanical Structures, Xi'an Jiaotong University, Xi'an, Shaan Xi, 710049, China.

Yuanhao Chen
School for Engineering of Matter, Transport & Energy, Arizona State University
Tempe, AZ, 85287, USA

ABSTRACT

In this paper, an improved model of cardiac conduction system with consideration of main pacemakers and heart muscles is investigated. The pacemakers consist of Sinoatrial node, atrioventricular node and His-Purkinje are simulated through three modified van der Pol oscillators with time delayed velocity coupling. The atrial and ventricular muscles are modeled by four modified Hindmarsh-Rose (HR) neuron systems stimulated by pacemakers. The synthetic electrocardiogram (ECG) constructed through a combination of electric signals of atrial and ventricular muscles. An implicit mapping topology for the complex cardiac firing is established. A specific Poincare section is defined to predict the waveform bifurcations varying with a system parameter the corresponding stability is defined by eigenvalue analysis. The cardiac firing results are presented to provide the normal and pathological rhythms in the cardiac conduction system. The presented study provides a new perspective in exploring the nonlinear dynamics of heart beating.

INTRODUCTION

The heart located in the chest is the power organ of the vascular system. It is divided into four cavities: left atrium, right atrium, left and right ventricles. The nonlinear dynamic analysis of the heart is of great significance to human life and health. The cardiac conduction system responsible for the expansion and contraction of the heart can be considered as a self-excited pacing network, in which there are three pacing nodes including Sinoatrial node (SA node), atrioventricular node (AV node) and His-Purkinje (HP) that are capable of spontaneously generating electrical pulses. The SA node has the highest natural frequency with a rate of 60-80 beats per minute (bpm), the AV node takes the second place at a rate of 40-60 bpm and His-Purkinje has the lowest natural frequency with about 20-40 bpm.

The electrical signals generated mainly by the SA node is transmitted to the atrium and then causes atrial contraction. The blood in the atrium will be pumped into the ventricle. When the electrical signal is transmitted through the three muscle fiber bundles to the atrioventricular node, it will pass a certain delay time. The lag phenomenon makes the ventricular fully dilated, then the electrical signals through the atrioventricular bundle to the ventricle, and then caused ventricular contraction, the ventricular blood pump out of the heart, so as to complete a heartbeat activity. Electrocardiogram (ECG), a combined record of the action potential waves through cardiac muscle tissue, contains P wave, QRS complex and T wave, which are associated with the SA node, AV node and HP activity respectively.

For the dynamic modeling of the electrical processes in the heart, various modeling approaches with different levels of details have been proposed and utilized. The majority of the models describe propagation of the action potentials on the cellular or tissue level cardiomyocytes [1]. However, the numerous computational resources are required to solve a lot of equations with many parameters for ionic currents in cell membranes. In this regard, a set of ordinary differential equations describing heartbeat dynamics without considering cardiac structure can reduce computation complexity and provide the necessary numerical information for the nonlinear dynamic analysis.

In 1928, van der Pol and van der Mark [2] first considered the heart as a system of coupled nonlinear oscillators and established three coupled electronic systems through equivalent circuits to simulate heart beating. However, their research only considered unidirectional coupling of pacing centers rather than bidirectional coupling under which the SA node may be affected physiologically by the AV node. Since the model of van der Pol and van der Mark, many authors tried to study the dynamics of the heart beating based on the van der Pol (VDP) model. Guevara and Glass [3] and West et al. [4] assumed a

[1] Contact author: xuyeyin@xjtu.edu.cn

bidirectional coupling exists between the SA and AV node and described the model of heart beating as two autonomous oscillators. Diego et al. [5] developed a new model of two nonlinear coupled oscillators as an equivalent circuit to describe the interaction between the SA and AV node and performed a bifurcation analysis. Elena Ryzhii and Maxim Ryzhii [6] presented a novel model of cardiac conduction system including main pacemakers described by improved VDP equations and heart muscles described by modified FitzHugh-Nagumo (FHN) models. They obtained synthetic ECG and reproduced several normal and pathological rhythms by means of clinically comparable realistic ECG signals. Foukou et al. [7] modeled the cardiac conduction systmen as a model of three nonlinear Grudzinsky-Zebrowsky type oscillators coupled by delayed connections and subjected to external stimuli. They confirmed the dynamics behaviors of pathological based on the maximum Lyapunov exponents.

The use of traditional numerical methods, such as the Runge-Kutta method or linear multi-step method, cannot achieve unstable periodic firing in the van der Pol equations. And because of the fast and slow motions of van der Pol oscillation, the generalized harmonic balance method is not enough to determine the complex periodic firings and quasi-periodic firings in nonlinear systems. For a more practical method for nonlinear dynamic problems, in 2015, Luo [8-9] developed a discrete mapping method that discretizes the continuous nonlinear system to build mappings for periodic motions. In 2018, Xu and Luo [10-13] employed the discrete mapping method to investigated van der Pol oscillators. A sequence from periodic motion-(2^m-1) to chaos was achieved and a series of symmetric and unsymmetric periodic motions to chaos was presented in a 2DOF Van der Pol Duffing oscillator. The semi-analytical bifurcation trees of stable and unstable periodic firings were obtained. Xing and Luo [14] applied the discrete mapping method in the Rossler system which is autonomous to present the period-1 motions to Twin Spiral homoclinic orbits.

In this paper, the van der Pol equations with unidirectional time-delayed coupling are adopted to simulate the action potential of three pacemakers. The Hindmarsh-Rose (HR) models [15] instead of FHN models simulate the electrical signals of cardiac muscles in order to present some biological characteristics, such as bursting. The numerical results of action potentials are obtained to describe the normal and pathological rhythms. Then the implicit mapping topology is established and the Poincare section is selected for dynamic prediction and stability analysis.

THE APPLICATION OF DISCRETE MAPPING METHOD

The action potential waveforms of the three natural pacemakers are described by the three modified asymmetric van der Pol equations with unidirectional time-delay velocity coupling, expressed by the state equations as [6]

$$\begin{aligned}
\dot{x}_1 &= x_2 \\
\dot{x}_2 &= -a_1 x_2 (x_1 - u_{11})(x_1 - u_{12}) - f_1 x_1 (x_1 + d_1)(x_1 + e_1) \\
\dot{x}_3 &= x_4 \\
\dot{x}_4 &= -a_2 x_4 (x_3 - u_{21})(x_3 - u_{22}) - f_2 x_3 (x_3 + d_2)(x_3 + e_2) \\
&\quad + K_{SA-AV}(x_2^{\tau} - x_4) \\
\dot{x}_5 &= x_6 \\
\dot{x}_6 &= -a_3 x_6 (x_5 - u_{31})(x_5 - u_{32}) - f_3 x_5 (x_5 + d_3)(x_5 + e_3) \\
&\quad + K_{AV-HP}(x_4^{\tau} - x_6)
\end{aligned} \tag{1}$$

where the pairs of variables (x_1, x_2), (x_3, x_4) and (x_5, x_6) refer to the SA node, AV node and Purkinje's fiber, respectively. u_{i1} and u_{i2} which have opposite signs to maintain relaxation oscillation characteristics are control parameters of heart beating; f_i represent the natural frequency of the three pacemakers; the parameters a_i, d_i and e_i are selected with shapes close to experimental data on action potentials of real pacemakers; k_{SA-AV} and k_{AV-HP} represent the unidirectional coupling coefficients between the pacemakers; $x_i^{\tau} = x_i(t-\tau)$ are the velocity coupling components of the time-delay signal which describes the lag phenomenon. (i=1,2,3)

Compared with the properties of the pacemaker cells, cardiac muscle cells do not demonstrate self-oscillatory behavior. Given the property, the model with positive product $u_{i1}u_{i2}$ is essential to adequately describe electrical response stimulated by the pacemakers. In this paper, consider four HR models to simulate the atrial and ventricular muscles as

$$\begin{aligned}
\dot{x}_7 &= k_1(-c_1 x_7 (x_7 - w_{11})(x_7 - w_{12}) - b_1 x_8 - dd_1 x_7 x_8 \\
&\quad + \frac{k_{ATDe} x_2}{1 + e^{-x_2}}) - x_9 \\
\dot{x}_8 &= k_1 h_1 (x_7 - g_1 x_8) \\
\dot{x}_9 &= r_1 (s_1 (x_7 - x70) - x_9)
\end{aligned}$$

$$\begin{aligned}
\dot{x}_{10} &= k_2(-c_2 x_{10} (x_{10} - w_{21})(x_{10} - w_{22}) - b_2 x_{11} - dd_2 x_{10} x_{11} \\
&\quad - \frac{k_{ATRe} x_2}{1 + e^{x_2}}) - x_{12} \\
\dot{x}_{11} &= k_2 h_2 (x_{10} - g_2 x_{11}) \\
\dot{x}_{12} &= r_1 (s_1 (x_{10} - x70) - x_{12})
\end{aligned} \tag{2}$$

$$\begin{aligned}
\dot{x}_{13} &= k_3(-c_3 x_{13} (x_{13} - w_{31})(x_{13} - w_{32}) - b_3 x_{14} - dd_3 x_{13} x_{14} \\
&\quad + \frac{k_{VNDe} x_6}{1 + e^{-x_6}}) - x_{15} \\
\dot{x}_{14} &= k_3 h_3 (x_{13} - g_3 x_{14}) \\
\dot{x}_{15} &= r_1 (s_1 (x_{13} - x70) - x_{15})
\end{aligned}$$

$$\dot{x}_{16} = k_4(-c_4 x_{16}(x_{16}-w_{41})(x_{16}-w_{42}) - b_4 x_{16} - dd_4 x_{16} x_{17} - \frac{k_{VNRe} x_6}{1+e^{x_6}}) - x_{18}$$
$$\dot{x}_{17} = k_4 h_4 (x_{16} - g_4 x_{17})$$
$$\dot{x}_{18} = r_1 (s_1 (x_{16} - x70) - x_{18})$$

Here (x_7,x_8,x_9), (x_{10},x_{11},x_{12}), (x_{13},x_{14},x_{15}) and (x_{16},x_{17},x_{18}) represent P wave, Ta wave, QRS wave and T wave, respectively. k_i are the scaling coefficients, the parameters c_i, w_{i1}, w_{i2}, b_i, h_i and dd_i are set to match real action potential waveforms of atrial and ventricular. (i=1,2,3,4)

Then ECG signals are obtained by integrating the atrial and ventricular muscles,

$$ECG = x_0 + x_7 - x_{10} + x_{13} + x_{16} \tag{3}$$

The parameter x_0 provides zero baseline of ECG signal.

The nonlinear dynamic models describing the conduction process of cardiac electrical signals have been established above and then dynamic analysis will be performed. Since Eq. (1) is not affected by the calculation results of Eq. (2), the dynamics of Eq. (1) can be discussed separately. Afterwards, the characteristics of the synthetic ECG can be analyzed based on the data obtained from the results of Eq. (1).

First, although the model is an autonomous system, a small time interval can be considered and then Eq. (1) can be discretized with a midpoint scheme as:

$$\begin{aligned}
x_{1,k} &= x_{1,k-1} + h x_{2,kc} \\
x_{2,k} &= x_{2,k-1} + h(-a_1 x_{2,kc}(x_{1,kc}-u_{11})(x_{1,kc}-u_{12}) \\
&\quad - f_1 x_{1,kc}(x_{1,kc}+d_1)(x_{1,kc}+e_1)) \\
x_{3,k} &= x_{3,k-1} + h x_{4,kc} \\
x_{4,k} &= x_{4,k-1} + h(-a_2 x_{4,kc}(x_{3,kc}-u_{21})(x_{3,kc}-u_{22}) \\
&\quad - f_2 x_{3,kc}(x_{3,kc}+d_2)(x_{3,kc}+e_2) + K_{SA-AV}(x^{\tau}_{2,kc} - x_{4,kc})) \\
x_{5,k} &= x_{5,k-1} + h x_{6,kc} \\
x_{6,k} &= x_{6,k-1} + h(-a_3 x_{6,kc}(x_{5,kc}-u_{31})(x_{5,kc}-u_{32}) \\
&\quad - f_3 x_{5,kc}(x_{5,kc}+d_3)(x_{5,kc}+e_3) + K_{AV-HP}(x^{\tau}_{4,kc} - x_{6,kc}))
\end{aligned} \tag{4}$$

where h is also variable for an autonomous system and

$$x_{i,kc} = \frac{x_{i,k} + x_{i,k-1}}{2}, (i = 1,2,3,4,5,6), k = 1,2,\ldots,mN \tag{5}$$

For the time-delay terms, the simple Lagrange interpolation is applied to determine the time-delay nodes

$$\begin{aligned}
x^{\tau}_{2,k} &= x_{2,k-l_k-1} + (1 - \frac{\tau}{h} + l_k)(x_{2,k-l_k} - x_{2,k-l_k-1}) \\
x^{\tau}_{4,k} &= x_{4,k-l_k-1} + (1 - \frac{\tau}{h} + l_k)(x_{4,k-l_k} - x_{4,k-l_k-1})
\end{aligned} \tag{6}$$

where $l_k = \mathrm{int}(\tau / h)$.

The mapping structure in Eq.(4) defines the mapping as $P_k: \mathbf{x}_{k-1} \to \mathbf{x}_k$ ($\mathbf{x}_k = (x_{1,k}, x_{2,k}, x_{3,k}, x_{4,k}, x_{5,k}, x_{6,k})^{\mathrm{T}}$, $k = 1,2,\cdots,mN$). For nonlinear solutions of the coupled van der Pol oscillators, the global mappings have the form

$$\begin{aligned}
&P_1 : \mathbf{x}_0 \to \mathbf{x}_1 \Rightarrow \mathbf{x}_1 = P_1 \mathbf{x}_0 \\
&P_2 : \mathbf{x}_1 \to \mathbf{x}_2 \Rightarrow \mathbf{x}_2 = P_2 \mathbf{x}_1 \\
&\vdots \\
&P_N : \mathbf{x}_{N-1} \to \mathbf{x}_N \Rightarrow \mathbf{x}_N = P_N \mathbf{x}_{N-1}
\end{aligned} \tag{7}$$

consider a mapping structure of $P = P_N \circ P_{N-1} \circ \cdots \circ P_2 \circ P_1$, where ' $\circ$ ' represents the action between mappings. The corresponding algebraic equations of the mapping structure are in Eq.(4):

$$\mathbf{g}_k(\mathbf{x}_{k-1}, \mathbf{x}_{1,k-1}, h) = \mathbf{0} \ (k = 1,2,\cdots mN) \tag{8}$$

where $\mathbf{g}_k = (g_{x_1,k}, g_{x_2,k}, g_{x_3,k}, g_{x_4,k}, g_{x_5,k}, g_{x_6,k})^{\mathrm{T}}$ with

$$\begin{aligned}
g_{1,k} &= x_{1,k} - x_{1,k-1} - h x_{2,kc} \\
g_{2,k} &= x_{2,k} - x_{2,k-1} - h(-a_1 x_{2,kc}(x_{1,kc}-u_{11})(x_{1,kc}-u_{12}) \\
&\quad - f_1 x_{1,kc}(x_{1,kc}+d_1)(x_{1,kc}+e_1)) \\
g_{3,k} &= x_{3,k} - x_{3,k-1} - h x_{4,kc} \\
g_{4,k} &= x_{4,k} - x_{4,k-1} - h(-a_2 x_{4,kc}(x_{3,kc}-u_{21})(x_{3,kc}-u_{22}) \\
&\quad - f_2 x_{3,kc}(x_{3,kc}+d_2)(x_{3,kc}+e_2) + K_{SA-AV}(x^{\tau}_{2,kc} - x_{4,kc})) \\
g_{5,k} &= x_{5,k} - x_{5,k-1} - h x_{6,kc} \\
g_{6,k} &= x_{6,k} - x_{6,k-1} - h(-a_3 x_{6,kc}(x_{5,kc}-u_{31})(x_{5,kc}-u_{32}) \\
&\quad - f_3 x_{5,kc}(x_{5,kc}+d_3)(x_{5,kc}+e_3) + K_{AV-HP}(x^{\tau}_{4,kc} - x_{6,kc}))
\end{aligned} \tag{9}$$

The periodicity condition of period-m waveforms is:

$$\begin{aligned}
&\mathbf{x}_{mN} = \mathbf{x}_0 \\
&\Rightarrow (x_{1,mN}, x_{2,mN}, x_{3,mN}, x_{4,mN}, x_{5,mN}, x_{6,mN})^{\mathrm{T}} \\
&= (x_{1,0}, x_{2,0}, x_{3,0}, x_{4,0}, x_{5,0}, x_{6,0})^{\mathrm{T}}
\end{aligned} \tag{10}$$

The initial conditions on the selected Poincare section as

$$x_{3,0} + x_{5,0} = 0 \tag{11}$$

The semi-analytical solutions of period-m waveforms in the nonlinear coupled van der Pol oscillators system can be achieved by solving the $6(mN+1)+1$ equations in Eq. (8), Eq. (10) and (11). Once the semi-analytical solutions of periodic waveforms are obtained, the stability and bifurcation analysis can be conducted by eigenvalue analysis.

Consider the perturbed equation of the discretized system as

$$\sum_{j=k-1}^{k} \frac{\partial \boldsymbol{g}_k}{\partial \boldsymbol{x}_j^{(m)}} \Delta \boldsymbol{x}_j^{(m)} + \frac{\partial \boldsymbol{g}_k}{\partial \boldsymbol{x}_j^{\tau(m)}} \left(\frac{\partial \boldsymbol{x}_j^{\tau(m)}}{\partial \boldsymbol{x}_{r_j}^{(m)}} \Delta \boldsymbol{x}_{r_j}^{(m)} + \frac{\partial \boldsymbol{x}_j^{\tau(m)}}{\partial \boldsymbol{x}_{r_j-1}^{(m)}} \Delta \boldsymbol{x}_{r_j-1}^{(m)} \right) = 0 \tag{12}$$

where $r_j = j - l_j$.

For the time-delayed nonlinear dynamical systems, a set of vectors is defined as

$$\begin{aligned}
\mathbf{y}_k^{(m)} &= (\mathbf{x}_k^{(m)}, \mathbf{x}_{k-1}^{(m)}, \cdots, \mathbf{x}_{r_{k-1}}^{(m)})^T, \\
\mathbf{y}_{k-1}^{(m)} &= (\mathbf{x}_{k-1}^{(m)}, \mathbf{x}_{k-2}^{(m)}, \cdots, \mathbf{x}_{r_{k-1}-1}^{(m)})^T, \\
\Delta\mathbf{y}_k^{(m)} &= (\Delta\mathbf{x}_k^{(m)}, \Delta\mathbf{x}_{k-1}^{(m)}, \cdots, \Delta\mathbf{x}_{r_{k-1}}^{(m)})^T, \\
\Delta\mathbf{y}_{k-1}^{(m)} &= (\Delta\mathbf{x}_{k-1}^{(m)}, \Delta\mathbf{x}_{k-2}^{(m)}, \cdots, \Delta\mathbf{x}_{r_{k-1}-1}^{(m)})^T,
\end{aligned} \tag{13}$$

The resultant Jacobian matrix of the period-m motion is

$$\begin{aligned}
DP &= DP_{mN} \cdot DP_{mN-1} \cdot \ldots \cdot DP_2 \cdot DP_1 \\
&= \left[\frac{\partial \mathbf{y}_{mN}}{\partial \mathbf{y}_0} \right]_{(\mathbf{x}_{mN}^*, \mathbf{x}_{N-1}^*, \cdots, \mathbf{x}_0^*,)} \\
&= \prod_{k=mN}^{1} \left[\frac{\partial \mathbf{y}_k}{\partial \mathbf{y}_{k-1}} \right]_{(\mathbf{x}_{k-1}^*, \mathbf{x}_k^*)}
\end{aligned} \tag{14}$$

and the linearized equation of the discrete mapping structure is

$$\Delta\mathbf{y}_{mN} = DP\Delta\mathbf{y}_0 = \underbrace{DP_{mN} \cdot DP_{mN-1} \cdot \ldots \cdot DP_2 \cdot DP_1}_{mN-\text{multiplication}} \Delta\mathbf{y}_0 \tag{15}$$

where

$$DP_k = \begin{bmatrix} \mathbf{B}_k^{(m)} & (\mathbf{a}_{k(r_{k-1}-1)}^{(m)})_{2\times 2} \\ \mathbf{I}_k^{(m)} & \mathbf{0}_k^{(m)} \end{bmatrix}_{2(s+1)\times 2(s+1)}, s = 1 + l_{k-1} \tag{16}$$

$$\begin{aligned}
\mathbf{B}_k^{(m)} &= \left[(\mathbf{a}_{k(k-1)}^{(m)})_{2\times 2}, \mathbf{0}_{2\times 2}, \cdots, (\mathbf{a}_{k(r_k-1)}^{(m)})_{2\times 2} \right], \\
\mathbf{I}_k^{(m)} &= diag(\mathbf{I}_{2\times 2}, \mathbf{I}_{2\times 2}, \cdots, \mathbf{I}_{2\times 2})_{2s\times 2s}, \\
(\mathbf{0}_k^{(m)})^{\mathbf{T}} &= (\mathbf{0}_{2\times 2}, \mathbf{0}_{2\times 2}, \cdots, \mathbf{0}_{2\times 2})_{2\times 2s}; \\
\mathbf{a}_{kj}^{(m)} &= \left[\frac{\partial \mathbf{g}_k}{\partial \mathbf{x}_k^{(m)}} \right]^{-1} \frac{\partial \mathbf{g}_k}{\partial \mathbf{x}_j^{(m)}}, \\
\mathbf{a}_{kr_j}^{(m)} &= \left[\frac{\partial \mathbf{g}_k}{\partial \mathbf{x}_k^{(m)}} \right]^{-1} \sum_{\alpha=j}^{j+1} \frac{\partial \mathbf{g}_k}{\partial \mathbf{x}_\alpha^{\tau(m)}} \frac{\partial \mathbf{x}_\alpha^{\tau(m)}}{\partial \mathbf{x}_{r_j}^{(m)}}, \\
\mathbf{a}_{k(r_j-1)}^{(m)} &= \left[\frac{\partial \mathbf{g}_k}{\partial \mathbf{x}_k^{(m)}} \right]^{-1} \sum_{\alpha=j-1}^{j} \frac{\partial \mathbf{g}_k}{\partial \mathbf{x}_\alpha^{\tau(m)}} \frac{\partial \mathbf{x}_\alpha^{\tau(m)}}{\partial \mathbf{x}_{r_j-1}^{(m)}}, \\
j &= k-1, k
\end{aligned}$$

The stability and bifurcations of the discrete nonlinear heart beating system can be determined by the eigenvalues of DP

$$\left| DP - \lambda \mathbf{I}_{2(s+1)\times 2(s+1)} \right| = 0 \tag{17}$$

The stability conditions are defined from the *discrete mapping method*[8-9].

i. If all eigenvalues of DP are within the unit circle (i.e. $|\lambda_i| < 1, i = \{1, 2, \ldots, 2(s+1)\}$), the period-m waveforms is stable.

ii. If at least one eigenvalue is out of the unit circle (i.e. $|\lambda_i| > 1, i \in \{1, 2, \ldots, 2(s+1)\}$), the period-m waveforms is unstable.

iii. When there are eigenvalues on the unit circle (i.e. $|\lambda_i| = 1$, $i \in \{1, 2, \ldots, 2(s+1)\}$), bifurcation analysis is necessary for the nonlinear heat beating system.

The bifurcations are defined as

iv. If $\lambda_i = 1$ with $\lambda_j | < 1$ ($i, j \in \{1, 2, \ldots, 2(s+1)\}, i \neq j$), saddle-node bifurcation (SN) occurs.

v. If $\lambda_i = -1$ with $|\lambda_j| < 1$ ($i, j \in \{1, 2, \ldots, 2(s+1)\}, i \neq j$), period-doubling bifurcation (PD) occurs.

vi. If $|\lambda_{i,j}| = 1$ ($i, j \in \{1, 2, \ldots, 2(s+1)\}$), $\lambda_i = \overline{\lambda}_j$), Neimark bifurcation (NB) occurs.

NUMERICAL RESULTS

From the reference [6], consider the values of parameters under normal heartbeat as: a_1 = 40, a_2 =a_3 =50; u_{11} = u_{21} =u_{31} = 0.83, u_{12} = u_{22} =u_{23} = -0.83; f_1 = 22, f_2 = 8.4, f_3 = 1.5; d_1 = d_2 = d_3 = 3, e_1 = 3.5, e_2 = 5, e_3 = 12; $K_{SA\text{-}AV}$ = $K_{AV\text{-}HP}$ = f_1; k_1 = 2e+3, k_2 = 400, k_3 = 1e+4, k_4 = 2e+2; $\tau = 0.5*(2.29/f_1 + 0.08)$; c_1 = c_2 = 0.26, c_3 = 0.12, c_4 = 0.1; w_{11} = 0.13, w_{12} = 1.0, w_{21} = 0.19, w_{22} = 1.0, w_{31} = 0.12, w_{32} = 1.1, w_{41} = 0.2, w_{42} = 0.8; h_1 = h_2 = 0.004, h_3 = h_4 = 0.008; b_1 = b_2 = b_4 = dd_1 = dd_2 = dd_4 = 0, b_3 = dd_3 = 0.015; g_1 = g_2 = g_3 = g_4 = 1.0; k_{ATDe} = k_{ATRe} = 4e-5, k_{VNDe} = 9e-5, k_{VNRe} = 6e-5; r_1 = 0.006, s_1 = 4.0, x_{70} = -1.6.

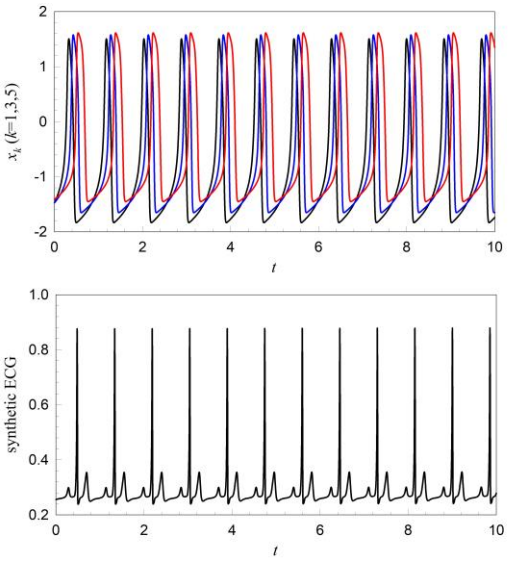

(a)

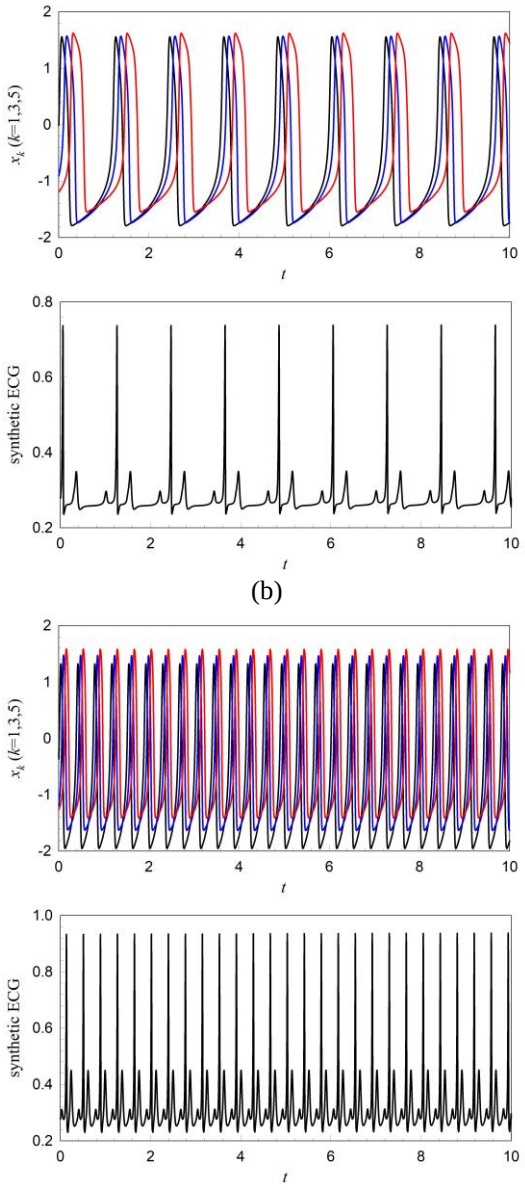

(b)

(c)

Fig.1 Time history diagram of three pacemakers and synthetic ECG (time interval h=0.001): (a) normal heartbeat rhythms at 70 bpm (f_1 = 22), (b) Sinus bradycardia at 43 bpm (f_1 = 13), (c) sinus tachycardia at 160 bpm (f1= 87).

In this part, the numerical simulations with different normal and pathological rhythms are performed. The figures demonstrate calculated action potentials of SA, AV and HP pacemakers and corresponding synthetic ECG waveforms. In the plots, the black curves x_1 represent the action potentials of SA pacemakers, the blue curves x_2 represent the action potentials of AV pacemakers and the red curves x_3 represent the action potentials of HP pacemakers.

In this part, the numerical simulations with different normal and pathological rhythms are performed. The figures demonstrate calculated action potentials of SA, AV and HP pacemakers and corresponding synthetic ECG waveforms. In the plots, the black curves x_1 represent the action potentials of SA pacemakers, the blue curves x_2 represent the action potentials of AV pacemakers and the red curves x_3 represent the action potentials of HP pacemakers.

In this part, the numerical simulations with different normal and pathological rhythms are performed. The figures demonstrate calculated action potentials of SA, AV and HP pacemakers and corresponding synthetic ECG waveforms. In the plots, the black curves x_1 represent the action potentials of SA pacemakers, the blue curves x_2 represent the action potentials of AV pacemakers and the red curves x_3 represent the action potentials of HP pacemakers.

Fig.1 depicts calculated action potentials response and synthetic ECG at different rhythms, which has been compared with real ECG in ref. [6]. For the normal case in Fig.1(a), all pacemakers are dominated by SA node and follow its rhythms of 70 bpm. The heart beat activity is completed approximately every 0.8 seconds. Action potentials appear in turn rather than synchronously due to the time delay phenomenon which fits with the real physiological situation. The sinus rhythm of sinus bradycardia is slower than 60 bpm. Fig.1(b) displays the longer heart beat periods and the lower amplitudes of ECG compared with the normal rhythm. At such slow rates the congestion of atrial and ventricular is not so sufficient that it may cause oxygen deficit. When SA node generates impulses greater than 100 bpm with other pacemakers synchronously following this rate, it is considered that sinus tachycardia shown in Fig.1(c) may appear. The waveforms remained consistent roughly but the action potentials of all pacemakers became shorter with the rate increase and the corresponding P-Ta and R-T interval became shorter.

When the frequency of sinus node is lower than normal frequency, the response to generate action potentials of the three pacemakers becomes asynchronous, as shown in figure 2. As can be seen from Fig.2(a), the generation frequency of the action potentials of the three pacemakers is inconsistent, which is because f1 is so small that the natural frequencies of the AV node and the HP pacemaker begin to play a dominant role in the heartbeat process.

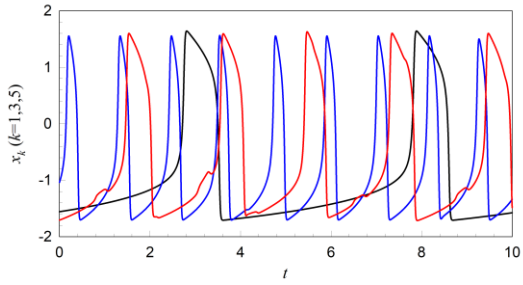

(a)

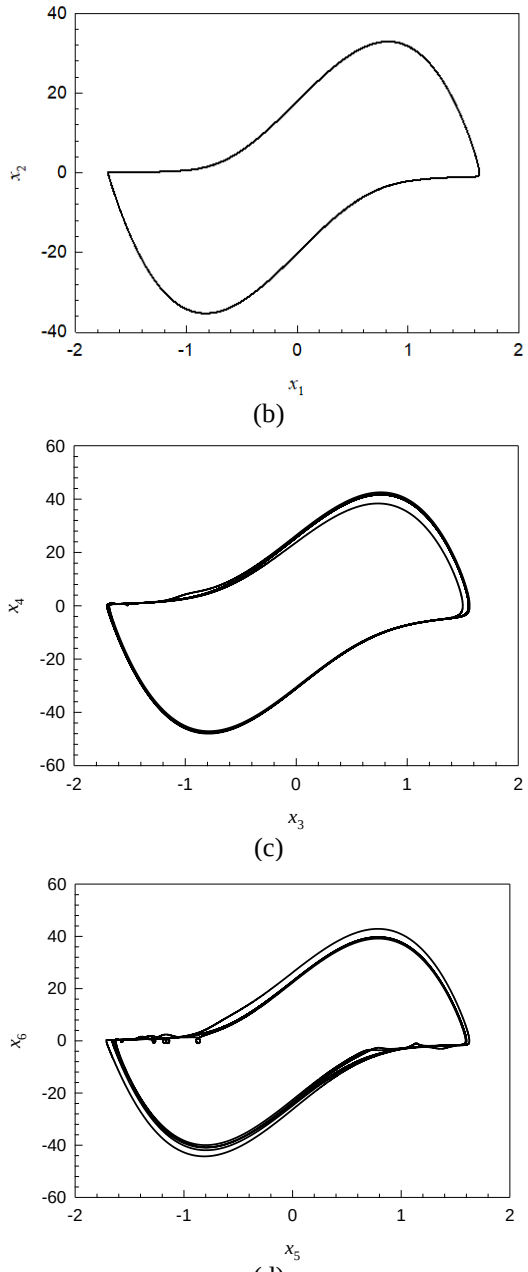

Fig.2 Time history diagram phase diagram of three pacemakers and (f_1=1.58, time interval h=0.001): (a)time series, (b) phase diagram, (x_1, x_2), (c) phase diagram, (x_3, x_4), (d) phase diagram, (x_5, x_6).

CONCLUSIONS

In this paper, the action potential waveforms of the nonlinear heart beating system based on three time-delayed coupled van der Pol equations and four HR models were investigated with the numerical midpoint method and the semi-analytical discrete implicit mapping method. The waveforms and phase diagrams of several arrhythmia were obtained. The eigenvalue analysis provides predictions for the occurrence of bifurcation points and stability switches in periodic waveforms within the corresponding parameter ranges. The stability provided data for such stimulus and help doctors avoid the unstable waveforms which are dangerous because of the continuous increasing amplitude and complex waveforms. This research presents a good scenario for nonlinear heart beating dynamics and has prospective applications in practical case. The nonlinear dynamics of cardiac system has complicated bifurcations of periodic waveforms which will be completed.

ACKNOWLEDGEMENT

This work is supported by the National Nature Science Foundation of China (Grant No. 12102319) and the Key R&D and Transformation Plan Project of Qinghai Province(NO. 2023-QY-215).

REFERENCES

[1] Fenton, Flavio, 2000, “Numerical Simulations of Cardiac Dynamics. What Can We Learn from Simple and Complex Models?”, In *Computers in Cardiology*. Vol. 27. pp: 251 - 254.

[2] van der Pol, Balth and Jan Van Der Mark, 1928 “LXXII. The heartbeat considered as a relaxation os cillation, and an electrical model of the heart”, *The London, Edinburgh, and Dublin Philosophical Magazine and Journal of Science*, **6**(38), pp: 763-775.

[3] Guevara, Michael R. and Leon Glass, 1982, “Phase locking, period doubling bifurcations and chaos in a mathematical model of a periodically driven oscillator: A theory for the entrainment of biological oscillators and the generation of cardiac dysrhythmias." *Journal of mathematical biology* , **14**, pp: 1-23.

[4] West, Bruce J., et al., 1985, “Nonlinear dynamics of the heartbeat: I. The AV junction: Passive conduit or active oscillator?”, *Physica D: Nonlinear Phenomena*, **17**(2), pp: 198-206.

[5] di Bernardo, Diego and Maria G. Signorini., 1998, “A model of two nonlinear coupled oscillators for the study of heartbeat dynamics”, *International journal of Bifurcation and Chaos*, **8**(10), pp: 1975-1985.

[6] Ryzhii E, Ryzhii M, 2014, “A heterogeneous coupled oscillator model for simulation of ECG signals”, Comput Methods Programs Biomed. 117(1), pp: 40-49.

[7] Fonkou, R. F. et al, 2023, “Dynamical behavior analysis of the heart system by the bifurcation structures.” Heliyon 9: n. pag.

[8] Luo, Albert Chao Jun, 2015, “Discretization and implicit mapping dynamics”, *Springer Berlin Heidelberg*.

[9] Luo, Albert Chao Jun, 2015, “Periodic flows to chaos based on discrete implicit mappings of continuous nonlinear systems”, *International. Journal of Bifurcation and Chaos*, **25**(3), pp:1550044.

[10] Xu, Yeyin, and Luo, Albert Chao Jun. “Sequent period-(2^m-1) motions to chaos in the van der Pol oscillator." *International Journal of Dynamics and Control*, **7,** pp: 795-807.

[11] Xu, Yeyin, and Luo, Albert. Chao. Jun, 2020, “Independent Period-2 Motions to Chaos in a van der Pol-Duffing Oscillator”, *International Journal of Bifurcation and Chaos*, **30**(15), pp:2030045.

[12] Xu, Yeyin, and Luo, Albert. Chao. Jun, 2019, “Frequency-amplitude characteristics of periodic motions in a periodically forced van der Pol oscillator”, *The European Physical Journal Special Topics*, **228**(9), pp:1839-1854.

[13] Xu, Yeyin, and Luo, Albert. Chao. Jun, 2019, “Sequent period-(2^m+1) motions to chaos in the van der Pol oscillator”, *International Journal of Dynamics and Control*, **7**(3), pp:795-807.

[14] Xing, S., and Luo, A. C. J. (May 4, 2023). "Period-1 Motions to Twin Spiral Homoclinic Orbits in the Rössler System." ASME. J. Comput. Nonlinear Dynam. August 2023; 18(8): 081008.

[15] Xu, Yeyin, and Wu, Ying. 2022, “Analytical predictions of stable and unstable firings to chaos in a Hindmarsh–Rose neuron system”, Chaos 1; 32 (11): 113113.